Mapping coastal ecosystems at very high temporal and high spectral resolutions using the maximum entropy classifier on 12-band Venμs and 8-band SuperDove imagery

Antoine Collin [1,2], Dorothée James [1,2], Laetitia Dupuy [3], Franck Dolique [3], Marion Jaud [4], Eric Feunteun [1,2]

[1] CGEL, EPHE-PSL University, 35800 Dinard, France – (antoine.collin; dorothee.james)@ephe.psl.eu
[2] BOREA, MNHN, Station Marine de Dinard, 38 Rue du Port Blanc, 35800 Dinard, France – eric.feunteun@mnhn.fr
[3] BOREA, Antilles University, Schoelcher, BP 7209 97275, France – (laetitia.dupuy; franck.dolique)@univ-antilles.fr
[4] UAR 3113, IUEM, Rue Dumont D'Urville, 29280 Plouzané, France – marion.jaud@univ-brest.fr

Keywords: Dune, Salt marsh, Mangrove, Seagrass, Coral, Maximum Entropy Classifier.

Abstract

Coastal landscapes are composed of littoral ecosystems in interaction with human societies. The ecosystem services delivered range from oxygen and soil production, food provisioning, ocean-climate regulation, to recreo-tourism activities. However, the sustainability of those air-land-sea interfaces are increasingly jeopardized by global changes and local stresses due to the anthropogenic drivers. The natural protection offered by those ecosystems to cope with the near future's sea-level rise and wind-wave intensification requires to be finely and precisely monitored.
High to very high spatial, spectral and temporal spaceborne observation constitutes a relevant solution to address this issue. However the trade-off in remote sensing constrains to emphasize one resolution at the detriment of the other ones. This research innovatively proposes to compare the classification (maximum entropy) performance, over five representative coastal landscapes, of two state-of-the-science satellite sensors provided with very high spectral and temporal resolutions along with a high spatial resolution, namely the 8-band SuperDove at 3 m, and the 12-band Venμs at 4 m.
Firstly, the addition of the intermediate visible and near-infrared bands to the standard blue-green-red dataset strongly improved the classification score of both SuperDove and Venμs orthorectified surface reflectance imageries: +8 and +7% for beach-dune, +18 and +4% for salt marsh, +2 and +1% for mangrove, +3 and +12% for seagrass, and +9 and +8% for coral, respectively. Secondly, the full optical SuperDove dataset outperformed the full optical Venμs dataset for salt marsh (3%), mangrove (3%) and coral reef (10%); but equalled it for the beach-dune (0%); and was outperformed for seagrass meadow (-4%). Both spatial and spectral resolutions (10 versus 12 bits for SuperDove and Venμs, respectively) were discussed to explain those findings.

1. Introduction

1.1 From Coastal Ecosystem Services to Nature-Based Solutions

Coastal ecosystems provide substantial services to humans living on the land-sea interface such as provisioning, regulation and cultural benefits (Barbier et al., 2011). Specifically, sandy beaches and dunes protect the shoreline by trapping sediment and dampening seaward wave and wind (James et al., 2024a). Muddy flats, salt marshes' and mangrove forests' vegetation diminish risks of salinization and erosion by expanding the natural land-sea buffer surface and reducing wave height (Collin et al., 2018a; Tieng et al., 2019). Seagrass meadows' vegetation attenuate erosion by slowing down the flow of circulation energy (James et al., 2024b). Honeycomb or coral reefs strongly wane coastal erosion and submersion by breaking the ocean waves (Collin et al., 2024a; Moussa et al., 2019). In addition, the vegetated blue carbon ecosystems sequester carbon at rates 10 times higher than those of terrestrial or tropical forests (Lochin et al., 2020), and the animal reefs multiply ecological niches, what dramatically fosters species richness, thus biodiversity (Collin et al., 2018b).

In a context of ocean-climate change and uncertainty, characterized by storm/cyclone intensification and sea-level rise, as well as human densification, featured with natural habitat degradation until destruction (Steffen et al., 2015), those living defences, coping with seaward risks, are now consensually recognized as nature-based adaptation solutions (Jordan and Fröhle, 2022).

1.2 Monitoring Coastal Ecosystems at Very High Spatial, Spectral and Temporal resolutions

As recommended by the Habitats-Fauna-Flora Directive from the European Commission, the surface and the biocenosis composition of those ecosystems constitute robust proxies for determining their health status. Recent remote sensing advances in both spatial and spectral domains appear as crucial tools to efficiently map those ecosystems in their spatial entirety along with the best taxonomic grain. Over the last decade, the spatial resolution of the coastal ecosystems' surveys has waxed from high (i.e., meter with spaceborne PlanetScope at 3 m, Collin et al., 2023), to very high (i.e., decimeter with spaceborne WorldView-3 at 0.3 m, Collin et al., 2019) until ultra high (i.e., centimeter with drone at 0.04 m, Collin et al., 2024b). In parallel, the spectral resolution also increased from the 8-band WorldView-3 at 0.3 m (Collin et al., 2021), to the 8-band SuperDove at 3 m (Collin et al., 2023), until the 12-band Sentinel-2 at 10 m (Collin et al., 2022). Fusion techniques based on machine learning are also increasingly developed to leverage high to very high spatial and spectral imageries for coastal ecosystem monitoring by, for examples, using a 12-band Sentinel-2-based imagery scaled at the 3-m SuperDove imagery (Collin et al., 2022), or working with a SuperDove-derived 8-band imagery scaled at the drone centimeter resolution (Collin et al., 2024b).

In addition, the individual plants and animal coastal colonies can rapidly shift their health status as a response of environmental (including anthropogenic) drivers. The

community of scientists, managers, policy and decision makers more often advocate to produce rich time-series, based on high to very high temporal resolution’s sensors, provided with also high to very high spatial and spectral capabilities, such as PlanetScope Superdove and Venμs satellite imagers.

1.2.1 SuperDove: The SuperDove sensor consists of the third generation of the PlanetScope constellation launched by the US company Planet Labs. In 2020, that constellation, also called PSB.SD, followed the first two constellations, named Dove-C (PS2) and Dove-R (PS2.SD), that were featured with four spectral bands: blue-green-red, and near-infrared. Since 29 April 2022, daily PlanetScope imageries are collected by the 8-band SuperDove CubeSats, whose number approximate 200 entities. Covering all terrestrial surface on Earth between 70° to -70° latitude, the Planet archive delivers very high spectro-temporal and high spatial resolution, since it is eight optical bands (from purple, 431 nm, to near-infrared, 885 nm) acquired at the day lag at 3 m pixel size.

1.2.2 Venμs: The space mission, launched in 2017, embodies a joint venture between the French and Israelian space agencies (namely, the Centre National d’Etudes Spatiales, CNES, and the Israeli Space Agency, ISA). The mission consists of a single super-spectral imager (12 bands), provided with a very high temporal (daily) and a high spatial resolution (4 m pixel size). The pushbroom camera was designed to discriminate vegetation health status and water quality by collecting 12 narrow bands from indigo (400 nm) to near-infrared (920 nm) with a 27-km swath. During the 5 commissioned years, the first phase, VM 1, surveyed 153 sites and the last phase, VM5, monitored 83 sites all over the world.

1.3 Comparing Coastal Classification Performances of Very High Temporal SuperDove and Venμs Sensors

The original research proposes to compare the mapping capabilities of five representative coastal landscapes from two state-of-the-science spaceborne sensors, namely SuperDove and Venμs, provided with high spatial and very high, both, spectral and temporal resolutions, what increased the likelihood to work with (almost) contemporary imageries for the same site. The main differences that distinguish those sensors is the spatial resolution (3 versus 4 m for SuperDove and Venμs, respectively), and the number of bands (correlated with the spectral resolution, 8 versus 12 optical bands for SuperDove and Venμs, respectively).

To optimize the susceptibility to get temporally-close SuperDove and Venμs imageries over the same coastal site, we focused on five VM5 sites, each displaying a representative coastal ecosystem: *Brest* in Brittany (France) for the beach-dune system (Figure 1a and 1f), *Vilaine* in Loire (France) for the estuary system provided with salt marshes and mud flats (Figure 1b and 1g), *UAECOA* in United Arab Emirates for the mangrove forests (Figure 1c and 1h), *Martiniq* in Caribbean Islands for the fringing reefs covered by seagrass meadows (Figure 1d and 1i), and *Lizardis* in Australia for the diversified coral reefs (Figure 1e and 1j).

The comparisons of the supervised classification performances will be quantified using an innovative learner, namely the maximum entropy learner. The principle of maximum entropy assumes that the probability distribution leading to the best classification is the one featured with the greatest diversity (that is to say, the largest entropy). The design experiments aim to measure the performances of (1) natural-colored (RGB), (2) visible and (3) optical (including near-infrared) datasets derived from each sensor, in order to compute the visible and optical contributions.

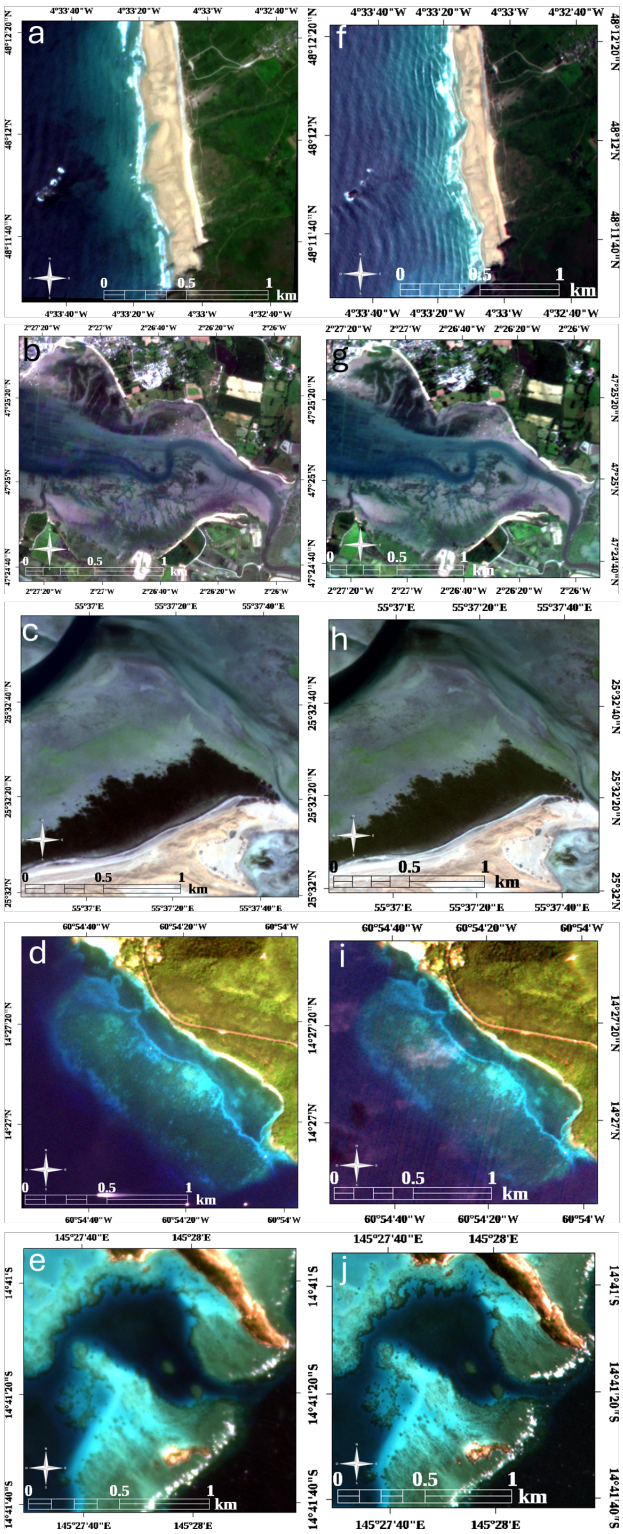

Figure 1. Natural-colored scenes of the five representative coastal ecosystems investigated through SuperDove (8-band at 3 m) and Venμs (12-band at 4 m) imageries: beach-dune system in Brittany (a and f), estuary system with mud flats and salt marshes in Loire (b and g), mangrove forests in United Arab Emirates (c and h), fringing reefs covered by seagrass meadows in Martinique (d and i), and coral reefs with barrier and fringing reefs with channel in Australia’s Great Barrier Reef (e and j).

2. Methodology

2.1 Study Sites

Five study sites were selected based on their occurrence in the SuperDove and Venμs (VM5) imagery archives: Brittany beach-dune system in Crozon’s peninsula (Figure 1a and f, N48°12’ W4°33’20’’); Loire’s neighbour estuary system with mud flats and salt marshes in Vilaine’s mouth (Figure 1b and 1g, N47°25’ W2°26’40’’); United Arab Emirates mangrove forests in Al-Sinniyah islands (Figure 1c and h, N25°32’30’’ E55°37’20’’); Le Marin fringing reefs with seagrass meadows in Martinique Island (Figure 1d and i, N14°27’ W60°54’30’’); and Australian complex landscape of coral reefs in Lizard Island (Figure 1e and j, S14°41’20’’ E145°27’80’’).

2.2 Satellite Imageries

2.2.1 SuperDove: Orbiting at 500 km, the latest PlanetScope CubeSats’ constellation daily samples the almost entire Earth’s land mass using 8 optical bands from 431 to 885 nm with a resampled 3 m pixel size (Table 1 and Figure 2). The average bandwidth of those bands is narrow, ranging from 21 nm for purple to 40 nm for near-infrared. The spectral performance of the SuperDove sensors surpass those of the Dove-C and Dove-R by adding the purple, Green I, yellow and red edge to the standard blue, green (II), red and near-infrared. The SuperDove imagery was selected on the Planet Explorer platform, for each site, by topping the area coverage at 100%, filtering the cloud cover to less than 10%, targeting the closest day to the Venμs imagery, and prioritizing a single than a multiple scene. Then, the selection was georectified online using rational polynomial coefficients, and radiometrically corrected at the surface reflectance (unitless), standardized to match that of Sentinel-2.

Band name	Band number	Center	Bandwidth	Min	Max
Purple	B1	441,5	21	431	452
Blue	B2	490	50	465	515
Green I	B3	531	36	513	549
Green II	B4	565	36	547	583
Yellow	B5	610	20	600	620
Red	B6	666	32	650	682
Red edge	B7	705	16	697	713
Near infrared	B8	865	40	845	885

Table 1. Spectral specificities of the SuperDove sensor.

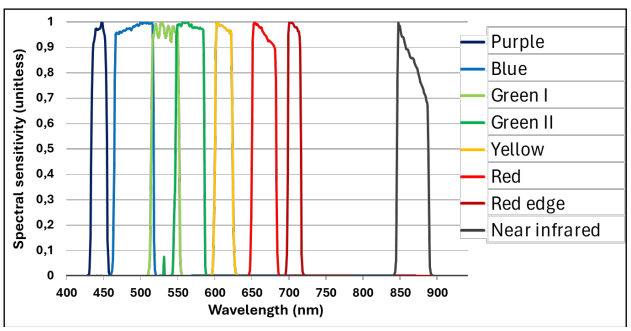

Figure 2. Lineplot of the PlanetScope SuperDove spectral properties.

The focused imageries were acquired on: 26-Jun-2024 for Brittany beach-dune system, 27-Jun-2024 for Loire’s neighbour estuary provided with mud flats and salt marshes, 03-Mar-2024 for United Arab Emirates’ mangrove forests, 01-Jan-2024 for Martinique’s fringing reefs covered by seagrass meadows, and 09-Jun-2024 for Australian coral reef island, respectively.

2.2.2 Venμs: The French-Israelian joint super-spectral sensor has captured 12 optical bands over the 83 VM5 sites from 400 to 920 nm with a resampled 4 m pixel size (Table 2 and Figure 3). The average bandwidth is as narrow as that of SuperDove, that it to say 32 nm, ranging from 16 nm for both near-infrared 1 and 2 to 40 nm for indigo, purple, blue, green, both yellows and near-infrared 3. De-commissioned in mid-2024, the unique sensor flew over the VM5 sites at 560 km altitude. For each site, the acquisition date was duly selected by keeping the imagery with no cloud cover. Then, the level 2 product was chosen since it is provided with an orthorectified surface reflectance, comparable with the SuperDove products.

Band name	Band number	Center	Bandwidth	Min	Max
Indigo	B1	420	40	400	440
Purple	B2	443	40	423	463
Blue	B3	490	40	470	510
Green	B4	555	40	535	575
Yellow 1	B5	620	40	600	640
Yellow 2	B6	620	40	600	640
Red	B7	667	30	652	682
Red edge	B8	702	24	690	714
Near infrared 1	B9	742	16	734	750
Near infrared 2	B10	782	16	774	790
Near infrared 3	B11	865	40	845	885
Near infrared 4	B12	910	20	900	920

Table 2. Spectral specificities of the Venμs sensor.

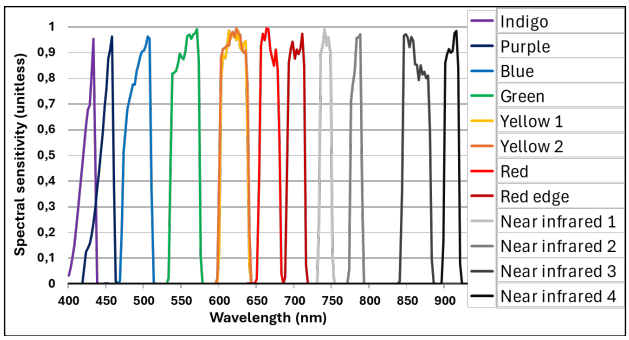

Figure 3. Lineplot of the Venμs spectral properties.

The imageries were collected on: 26-Jun-2024 for Brittany beach-dune system (same date as SuperDove), 27-Jun-2024 for Loire’s neighbour estuary provided with mud flats and salt marshes (same date as SuperDove), 03-Mar-2024 for United Arab Emirates’ mangrove forests (same date as SuperDove), 19-Dec-2023 for Martinique’s fringing reefs covered by seagrass meadows (11 difference days), and 10-Jun-2024 for Australian coral reef island (1 difference day).

2.3 Maximum Entropy Classification

The calibration and validation regions of interest were numerically selected for their property of purity, representative of the class. The polygons encompassed 1000 calibration and 500 validation pixels for each class for SuperDove. Since we used the same polygons, the Venμs dataset was composed of 568 calibration and 284 validation pixels for each class. The calibration sub-dataset trained the maximum entropy classifier and the classification performance was estimated using the confusion matrix applied to the validation sub-dataset, and summarized by the overall accuracy (OA).

2.3.1 Beach-dune system: Six classes were investigated (dry sand, wet sand, white dune, grey dune, tree, water).

2.3.2 Estuary system with mud flats and salt marshes: Nine classes were studied (immersed mud, emerged mud, immersed salt marsh, emerged salt marsh, soil, crop, tree, urban, water).

2.3.3 Mangrove forests: Seven classes were examined (immersed mud, emerged mud, seaweed, mangrove, dry sand, shrub, water).

2.3.4 Fringing coral reefs with seagrass meadows: Six classes were classified (coral reef, seagrass, immersed sand, dry sand, terrestrial vegetation, water).

2.3.5 Coral reef system: Eight classes were recognized (barrier reef, channel, fringing reef, immersed sand, wave, rock, terrestrial vegetation, water).

3. Results and Discussion

3.1 Coastscape Classification

The Figure 4 shows the overall performance (OA) for the five sites, each one analyzed by six spectral combinations: RGB, all visible, and all optical (including the near-infrared gamut) for both SuperDove and Venμs surface reflectance imageries.

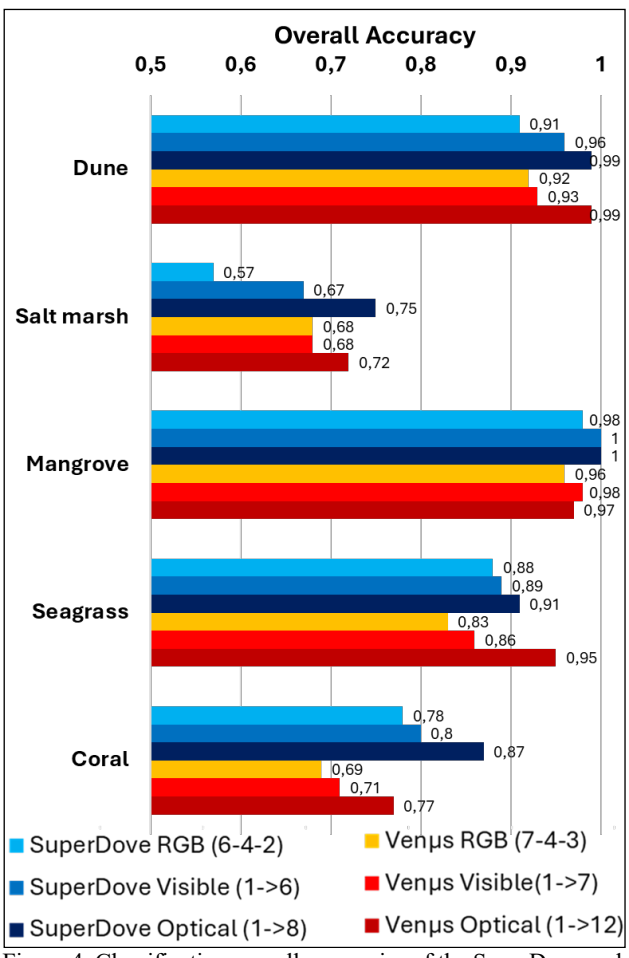

Figure 4. Classification overall accuracies of the SuperDove and Venμs spectral combinations tied to the five coastscapes.

Three distinct patterns can be drawn: (1) a gradient of classification performances across ecosystems, from salt marsh (57% OA) to mangrove (100% OA); (2) an increase in performance positively correlated with the addition of spectral bands, from RGB to all optical (infrared) through all visible combinations; and (3) a better overall performance of SuperDove compared to Venμs for four sites out of five (only salt marsh was better classified by Venμs).

The Table 3 further refines the predominance of SuperDove score compared to Venμs along an increasing gradient: salt marsh, dune, mangrove, seagrass and coral.

Coastscape	RGB	Visible	Optical
Dune	0,01	-0,03	0
Salt marsh	0,11	0,01	-0,03
Mangrove	-0,02	-0,02	-0,03
Seagrass	-0,05	-0,03	0,04
Coral	-0,09	-0,09	-0,1

Table 3. Venμs minus SuperDove difference in classification performance across the five coastal ecosystems.

Those findings, benefiting to SuperDove, might be partly explained by three aspects: (1) the spatial resolution, (2) the spectral resolution, and (3) the twin yellow band in Venμs. Even if the spatial resolution only differs from 1 m (3 m for SuperDove and 4 m for Venμs), this slight improvement in pixel size favours SuperDove since more pixels (thus, better learning) were used for the calibration process insofar as we used the same regions of interest. Prior to getting the surface reflectance product for both sensors, the radiometric resolution was also at the benefit of SuperDove, acquiring imagery at 12 bits (i.e., 4096 digital values for each band), whereas Venμs collected data at 10 bits (i.e., 1024 digital values for each band). That radiometric contrast might hinder the learning process of the classifier due to the coarser transmission in the atmosphere and hydrosphere tied to Venμs. Finally, Venμs imager comprises two yellow bands, both ranging from 600 to 640 nm, that were purposed to derive digital terrain model, because their opposite position in the focal plane enabled to get a 1.5° observation angle difference (Salvoldi et al., 2022). Even though that geometric specificity can generate promising relief results, the spatial discrepancy of the same electromagnetic radiation is likely to impede the learning process of the classifier. Further investigation will focus on that twin yellow effect related to Venμs.

3.2 Habitat-scale Classification

The series of the Figure 5 to Figure 9 represents the best classification product issued from the maximum entropy learner of the SuperDove and the Venμs surface reflectance imagery for each of the five studied coastscapes.

3.2.1 Beach-dune system: The Figure 5 highlights the best performance with all optical dataset for both SuperDove (Figure 5a, OA=99%) and Venμs (Figure 5b, OA=99%).

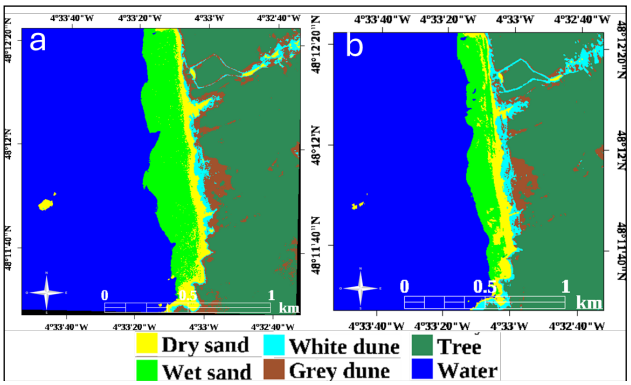

Figure 5. Maximum entropy classification maps of (a) the SuperDove optical dataset (OA=99%), and (b) the Venμs optical dataset (OA=99%).

3.2.2 Estuary system with mud flats and salt marshes: The Figure 6 shows the best performance with all optical dataset for both SuperDove (Figure 6a, OA=75%) and Venμs (Figure 6b, OA=72%).

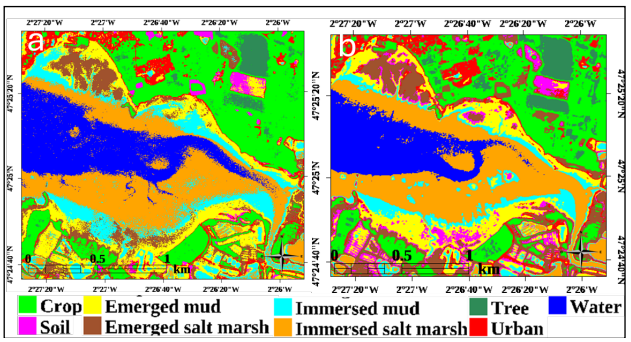

Figure 6. Maximum entropy classification maps of (a) the SuperDove optical dataset (OA=75%), and (b) the Venμs optical dataset (OA=72%).

3.2.3 Mangrove forests: The Figure 7 distincts the best performance with all optical dataset for SuperDove (Figure 7a, OA=100%) and only visible dataset for Venμs (Figure 7b, OA=98%).

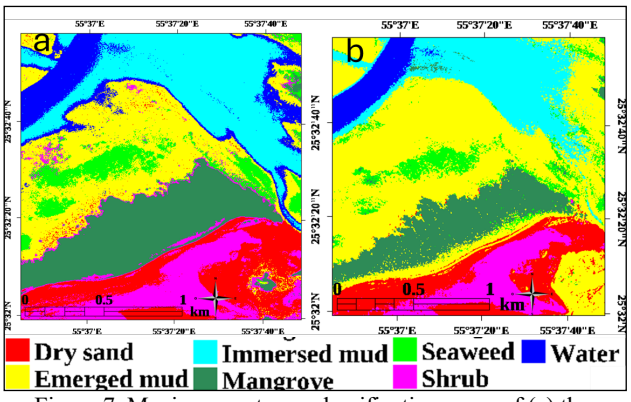

Figure 7. Maximum entropy classification maps of (a) the SuperDove optical dataset (OA=100%), and (b) the Venμs visible dataset (OA=98%).

3.2.4 Fringing coral reefs with seagrass meadows: The Figure 8 confirms the best performance with all optical dataset for both SuperDove (Figure 8a, OA=91%) and Venμs (Figure 8b, OA=95%).

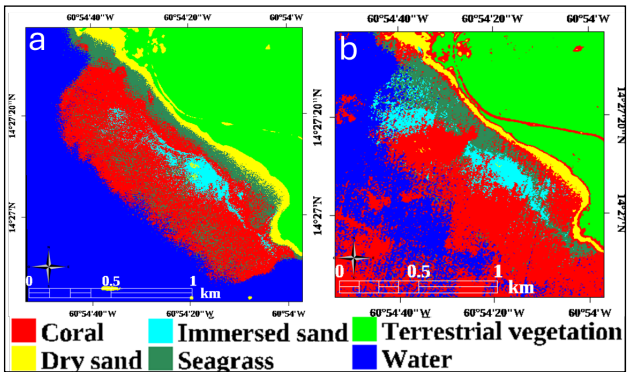

Figure 8. Maximum entropy classification maps of (a) the SuperDove optical dataset (OA=91%), and (b) the Venμs optical dataset (OA=95%).

3.2.5 Coral reef system: The Figure 9 displays the best performance with all optical dataset for both SuperDove (Figure 9a, OA=87%) and Venμs (Figure 9b, OA=77%).

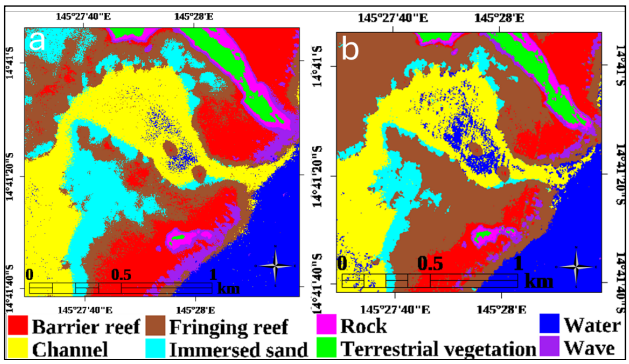

Figure 9. Maximum entropy classification maps of (a) the SuperDove optical dataset (OA=87%), and (b) the Venμs optical dataset (OA=77%).

4. Conclusion

An array of five representative coastal landscapes was satisfactorily classified by a maximum entropy learner trained and tested using the spaceborne 8-band SuperDove and the 12-band Venμs surface reflectance imagery at 3 and 4 m pixel size, respectively. Thanks to the very high temporal resolution characterizing those both sensors, a beach-dune system (in Brittany), an estuary featured with mud flats and salt marshes (in Loire), and a mangrove forest (in United Arab Emirates) were collected the same date, while a fringing reef with a seagrass meadow (in Martinique), and a coral reef island (in Australia) were acquired at 11 days and a single difference day, respectively.

Compared to the Venμs complete imagery, the SuperDove optical dataset better classified salt marsh (3%), mangrove (3%) and coral reef (10%); equalled performance for the beach-dune (0%); and underperformed for seagrass meadow (-4%). Both spatial and spectral resolutions (10 versus 12 bits for SuperDove and Venμs, respectively) can explain those findings.

It is important to underline the great increase in the classification performance by adding the intermediate visible and near-infrared bands to the standard blue-green-red dataset (+8 and +7% for beach-dune, +18 and +4% for salt marsh, +2 and +1% for mangrove, +3 and +12% for seagrass, and +9 and +8% for coral, associated with SuperDove and Venμs, respectively).

Acknowledgements

Authors gratefully acknowledge both (1) Planet Labs for the collection and provision of free SuperDove imageries through their basic education and research program, as well as (2) French and Israelian spatial agencies (CNES and ISA, respectively), for the acquisition and supply of free Venμs imageries.

References

Barbier, E.B., Hacker, S. D., Kennedy, C., Koch, E. W., Stier, A.C., Silliman, B.R., 2011: The value of estuarine and coastal ecosystem services. *Ecological monographs*, 81(2), 169-193.

Collin, A., Andel, M., Lecchini, D., Claudet., J., 2021 : Mapping Sub-Metre 3D Land-Sea Coral Reefscapes Using Superspectral WorldView-3 Satellite Stereoimagery. *Oceans*, 2(2), 315-329.

Collin, A., Dubois, S., Ramambason, C., Etienne, S., 2018b: Very high resolution mapping of emerging biogenic reefs using airborne optical imagery and neural network: the honeycomb worm (*Sabellaria alveolata*) case study. *International Journal Remote Sensing*, 39(17), 5660-5675.

Collin, A., James, D., Feunteun, E., 2022: Towards better coastal mapping using fusion of high temporal Sentinel-2 and PlanetScope-2 imageries: 12 bands at 3 m through neural network modelling. *Int. Arch. Photogramm. Remote Sens. Spatial Inf. Sci.*, XLIII-B3-2022, 479-484.

Collin, A., James, D., Gairin, E., Aubert, M., Daniel, Y., Feunteun, E., Dubois, S., 2024a: The Spatial Network of the Largest Honeycomb Reef in the World as Revealed by an Ultra-High Resolution Lidar Drone. *Journal of Coastal Research*, 113(sp1), 961-965.

Collin, A., James, D., Lesacher, M., Feunteun, E., 2024b. Ultra-High Resolution Temperature Mapping of the Muddy, Sandy, and Rocky Coasts using UAV-scaled SuperDove Imagery. Journal of Coastal Research, 113(sp1), 529-533.

Collin, A., Lambert, N., James, D., Etienne, S., 2018a: Mapping wave attenuation induced by salt marsh vegetation using WorldView-3 satellite imagery. *Revista de Investigación Marina*, 25(2), 67-69.

Collin, A., Palola, P., James, D., Pastol, Y., Monpert, C., Loyer, S., ..., Wedding, L., 2023: Superdove-modelled bathymetry using neural networks along a turbidity gradient: Bréhat, Saint-Barthélémy and Tetiaroa islands. *The International Archives of the Photogrammetry, Remote Sensing and Spatial Information Sciences*, 48, 1351-1356.

Collin, A.M., Andel, M., James, D., Claudet, J., 2019: The superspectral/hyperspatial WorldView-3 as the link between spaceborne and hyperspectral and airborne hyperspatial sensors: the case study of the complex tropical coast. *Int. Arch. Photogramm. Remote Sens. Spatial Inf. Sci.*, XLII-2/W13, 1849-1854.

James, D., Collin, A., Bouet, A., 2024b: Drone-Based Spatio-Temporal Assessment of a Seagrass Meadow: Insights into Anthropogenic Pressure. *Environmental Sciences Proceedings*, 29(1), 41.

James, D., Collin, A., Bouet, A., Perette, M., Dimeglio, T., Hervouet, G., ..., Lebas, J.F., 2024a: Multi-Temporal Drone Mapping of Coastal Ecosystems in Restoration: Seagrass, Salt Marsh, and Dune. *Journal of Coastal Research*, 113(sp1), 524-528.

Jordan, P., Fröhle, P., 2022: Bridging the gap between coastal engineering and nature conservation? A review of coastal ecosystems as nature-based solutions for coastal protection. *Journal of coastal conservation*, 26(2), 4.

Lochin, P., Collin, A., James, D., Pastol, Y., Costa, S., 2020: Blue carbon attenuation of future coastal risks related to extreme stream- and sea-water levels: the high-resolution 2D simulation as a management tool. *Revista de Investigación Marina*, 27(1), 47-50.

Moussa, R.M., Fogg, L., Bertucci, F., Calandra, M., Collin, A., Aubanel, A., ..., Planes, S., 2019: Long-term coastline monitoring on a coral reef island (Moorea, French Polynesia). *Ocean and Coastal Management*, 180, 104928.

Salvoldi, M., Cohen-Zada, A. L., Karnieli, A., 2022: Using the VENμS Super-Spectral Camera for detecting moving vehicles. *ISPRS Journal of Photogrammetry and Remote Sensing*, 192, 33-48.

Steffen, W., Broadgate, W., Deutsch, L., Gaffney, O., Ludwig, C., 2015: The trajectory of the Anthropocene: the great acceleration. *The anthropocene review*, 2(1), 81-98.

Tieng, T., Sharma, S., MacKenzie, R.A., Venkattappa, M., Sasaki, N.K., Collin, A., 2019: Mapping mangrove forest cover using Landsat-8 imagery, Sentinel-2, Very High Resolution Images and Google Earth Engine algorithm for entire Cambodia. *IOP Conference Series: Earth and Environmental Science*, 266(1), 012010.